

# **An assessment of structural enthalpy and crystallization pathways of $\text{Mg}_{65}\text{Zn}_{30}\text{Ca}_5$ bulk metallic glass and amorphous films**

**Scott Gleason, David Miskovic, Nicholas Hamilton, Kevin Laws, Michael Ferry**

UNSW Australia  
School of Material Science and Engineering

July 28, 2017

# ABSTRACT

The structural nature and thermal stability of amorphous alloys is highly dependent on the method by which they are produced, i.e. their relaxation rate upon cooling. Both bulk samples and metallic glass films of  $\text{Mg}_{65}\text{Zn}_{30}\text{Ca}_5$  were produced by copper mold casting and direct current (DC) magnetron sputtering onto aluminium substrates, respectively. Comparisons between structural enthalpy, crystallization pathways, relaxation and crystallization kinetics of the bulk samples and films were examined by elevated temperature XRD and DSC. Compared with equivalent experiments on the bulk alloy, results for the thin films show distinct differences in structural enthalpy and deviations from the expected crystalline phase evolution, displaying minor peak shifts, failure of some phases to evolve, and variations in the evolution rates.

# TABLE OF CONTENTS

<b>ABSTRACT</b>	<b>i</b>
<b>TABLE OF CONTENTS</b>	<b>1</b>
<b>1 INTRODUCTION</b>	<b>1</b>
<b>2 METHOD</b>	<b>1</b>
2.1 Master alloy . . . . .	1
2.2 DC magnetron sputtering . . . . .	1
2.3 Stylus profiler analysis . . . . .	2
2.4 EDS analysis . . . . .	2
2.5 DSC characterization . . . . .	2
2.6 XRD characterization . . . . .	2
<b>3 RESULTS</b>	<b>3</b>
<b>4 DISCUSSION</b>	<b>4</b>
<b>5 CONCLUSIONS</b>	<b>4</b>
<b>6 ACKNOWLEDGEMENTS</b>	<b>4</b>
<b>7 REFERENCES</b>	<b>4</b>

# 1 INTRODUCTION

The structural nature and thermal stability of amorphous alloys is highly dependent on the method by which they are produced, i.e. their relaxation rate upon cooling. Both bulk samples and metallic glass films of  $\text{Mg}_{65}\text{Zn}_{30}\text{Ca}_5$  were produced by copper mold casting and direct current (DC) magnetron sputtering onto aluminium substrates, respectively. Comparisons between structural enthalpy, crystallization pathways, relaxation and crystallization kinetics of the bulk samples and films were examined by elevated temperature XRD and DSC. Compared with equivalent experiments on the bulk alloy, results for the thin films show distinct differences in structural enthalpy and deviations from the expected crystalline phase evolution, displaying minor peak shifts, failure of some phases to evolve, and variations in the evolution rates.

Key sources <sup>Zhang Zhang Zhang 2012</sup> [1, 2] [3]

## 2 METHOD

### 2.1 Master alloy

The master alloy of  $\text{Mg}_{65}\text{Zn}_{30}\text{Ca}_5$  was produced using high-purity elements of Mg (99.85 wt%), Zn (99.995 wt%), and Ca (99.8 wt%). The alloy was prepared by induction melting in boron nitride coated graphite crucibles, purged with Ar (99.997 vol.% purity) five times, and protected with a circulating Ar atmosphere. Alloy homogeneity was ensured by heating and cooling through a cycle of 700°C, 385°C, 650°C, 385°C, 650°C to a casting temperature of 500 °C and 450°C for for injection and gravity casting respectively. Bulk amorphous  $\text{Mg}_{65}\text{Zn}_{30}\text{Ca}_5$  rod of 2.5mm diameter and plates of thickness of  $XX\mu\text{m}$  were produced by copper mold injection casting. The 25.4mm diameter targets were prepared from a cylindrical copper mold gravity castings sectioned to thicknesses of 3.25mm. All samples and targets were stored under Ar when not being examined or used.

### 2.2 DC magnetron sputtering

Films were produced from an in-house DC magnetron sputtering facility with Ar working gas (99.997 vol.% purity). The power was 15W, typical voltage of 290 – 350V, nominal chamber pressure of 1 bar, substrate temperature of 25 °C, and Ar flow of 3.01 SCCM. Films were deposited directly onto to Al DSC lid substrates. Depositions were for a period of 35 minutes. Deposition rate was estimated at 1.2nm/s.

## 2.3 Stylus profiler analysis

Nominal film thickness was measured by a stylus profiler (Dektak 2A, Bruker, Germany). A glass slide was placed under the substrates within the sputtering chamber, allowing the substrates to act as a mask. Profile measurements were taken by measuring the height difference between the bare glass and the film covered glass. This film thickness was used to estimate the sputter deposition rate.

## 2.4 EDS analysis

Alloy composition and homogeneity were confirmed by SEM-EDS (S3400, Hitachi, Japan). Hyper-maps were collected with an accelerating voltage of 15 – 20 kV, and a probe current of 50 nA.

## 2.5 DSC characterization

Isochronic DSC (204 F1 Phoenix, Netzsch, Selb, Germany) was carried out in Al crucibles under a protective Ar (99.997 vol.% purity) atmosphere. Scans were performed at heating rates of 5 to 100 K/min.

For annealed XRD the samples were heat treated in the DSC by heating to the desired temperature at 20 K/min followed by Ar quenching to room temperature.

## 2.6 XRD characterization

Annealing XRD (Empyrean, PANalytical, Cu  $K_{\alpha}$  X-ray source,  $\lambda = 1.541 \text{ \AA}$ ) was performed at room temperature. (Generator Voltage 45, Tube Current 40, Scan Step Size 0.0262606, Time per Step 397.29).

Dynamic XRD (D8, Bruker, Cu  $K_{\alpha}$  X-ray source,  $\lambda = 1.541 \text{ \AA}$ ) was performed by raising temperature at a rate of 20 K/min and performing scans *in situ*. The first scan was performed at 35 °C, then 75 °C, after which temperature was raised in 5 K increments. The  $2\theta$  scans from 31 – 60° were completed within 1092 sec (18 min, 12 sec) to minimise the effects of recrystallisation during the experiment. (Generator Voltage 45, Tube Current 100, Scan Step Size 0.02, Time per Step 134.4).

### 3 RESULTS

From the 35 minute depositions a nominal film thickness of  $2.5\mu\text{m}$  was obtained, giving a deposition rate of approximately  $1.2\text{nm/s}$ . The temperature within the chamber was found to rise  $3 - 4^\circ\text{C}$ , significantly less than the expected  $20\text{K}$  suggested by similar setups [4].

EDS analysis shows good agreement in the nominal composition for both the bulk and film  $\text{Mg}_{65}\text{Zn}_{30}\text{Ca}_5$ , see Table 1.

EDS Analysis	Bulk (at%)	Film (at%)
Mg	$64.85 \pm 3.18$	$62.92 \pm 3.24$
Zn	$29.55 \pm 0.82$	$31.17 \pm 0.95$
Ca	$5.60 \pm 0.17$	$5.91 \pm 0.19$

Table 1: EDS composition of bulk and film  $\text{Mg}_{65}\text{Zn}_{30}\text{Ca}_5$  in atomic weight percent.

Heating Rate $\beta$ $\text{K/min}$	$T_g$	$T_{x1}$	$T_{x2}$	$T_{x3}$	$T_{x4}$	$T_{x5}$
100	136.1	164.8	193.4	201.8	240.2	262.4
80	132.0	160.0	194.4	201.9	238.2	260.3
60	129.6	157.7	190.0	197.8	232.9	259.0
40	126.6	155.2	189.0	200.0	226.4	254.7
30	126.2	151.5	187.0	198.4	221.0	251.1
20	125.1	149.8	188.4	197.0	216.0	246.8
15	123.8	148.3	186.2	195.6	212.2	243.9
10	123.5	144.5	183.4	192.9	207.4	239.8
5	120.5	141.1	179.7	187.5	199.8	232.7

Table 2: Bulk  $\text{Mg}_{65}\text{Zn}_{30}\text{Ca}_5$  alloy onset temperatures for the various DSC heating rates  $\beta$ . All temperatures are in  $^\circ\text{C}$ .

Heating Rate $\beta$ $\text{K/min}$	$T_g$	$T_{x1}$	$T_{x2}$	$T_{x3}$	$T_{x4}$	$T_{x5}$
100	108.5	128.6		177.3		240.3
80	106.0	121.2		165.6		238.8
60	107.3	134.0		176.1		237.8
40	100.2	119.8		170.7		234.2
30	95.3	110.4		169.5		232.5
20	95.5	115.2		170.5		229.4
15	92.5	113.5		168.8		224.0

Table 3: Film  $\text{Mg}_{65}\text{Zn}_{30}\text{Ca}_5$  alloy onset temperatures for the various DSC heating rates  $\beta$ . All temperatures are in  $^\circ\text{C}$ .

Variable heating rate DSC for both the bulk and film  $\text{Mg}_{65}\text{Zn}_{30}\text{Ca}_5$  was used to establish the fragility of the system. Numerical solutions were used to fit the equation  $\beta^{-1} = \tau_0 e^{\left(\frac{D^* T_0}{T-T_0}\right)}$  [source] for both the bulk and film. The fragility  $m$  could then be calculated from the relationship  $D^* = 590/(m - 16)$  Shuai2014 [4, 5].

For the bulk it was found  $\beta^{-1} = 1.338E - 16e^{5274\left(\frac{1}{T-T_0}\right)}$  with Adj.  $R^2 = 0.972$ , giving a  $D^* = 20.4$ , and a fragility  $m = 44.9$ . For the film  $\beta^{-1} = 5.921E - 11e^{2766\left(\frac{1}{T-T_0}\right)}$  with Adj.  $R^2 = 0.861$ , giving a  $D^* = 10.0$ , and fragility  $m = 75.0$ . See Figure 5. [fig:Fragility\\_BulkFilm\\_mValue](#)

## 4 DISCUSSION

The use of a 60K DSC heating rate compared to the more commonly used 20K rate [sources] shifts peaks for the bulk  $\text{Mg}_{65}\text{Zn}_{30}\text{Ca}_5$  alloy about 8 - 15 degrees higher. This higher heating rates were used because crystallization events for the films were different to differentiation at the lower heating rate. Films show little shift to high temperature peaks with increases heating rates, but large shifts with relaxation. Bulk show the opposite behaviour, larger peaks shifts with higher heating rates and little shift with relaxation.

## 5 CONCLUSIONS

## 6 ACKNOWLEDGEMENTS

Yu Wang for his assistance with XRD experimentation and Rietveld refinement.

## 7 REFERENCES

- [1] Y. N. Zhang, G. J. Rocher, B. Briccoli, D. Kevorkov, X. B. Liu, Z. Altounian, and M. Medraj. Crystallization characteristics of the Mg-rich metallic glasses in the Ca-Mg-Zn system. *Journal of Alloys and Compounds*, 552:88–97, 2013.
- [2] Yi-Nan Zhang, Dmytro Kevorkov, Xue Dong Liu, Florent Bridier, Patrice Chartrand, and Mamoun Medraj. Homogeneity range and crystal structure of the  $\text{Ca}_2\text{Mg}_5\text{Zn}_{13}$  compound. *Journal of Alloys and Compounds*, 523:75–82, 2012.

hang2011

[3] Yi-Nan Zhang, Dmytro Kevorkov, Florent Bridier, and Mamoun Medraj. Experimental study of the Ca-Mg-Zn system using diffusion couples and key alloys. *Science and Technology of Advanced Materials*, 12(2):025003, 2011.

Wang2014

[4] J. Q. Wang, N. Chen, P. Liu, Z. Wang, D. V. Louzguine-Luzgin, M. W. Chen, and J. H. Perepezko. The ultrastable kinetic behavior of an Au-based nanoglass. *Acta Materialia*, 79(0):30–36, 2014.



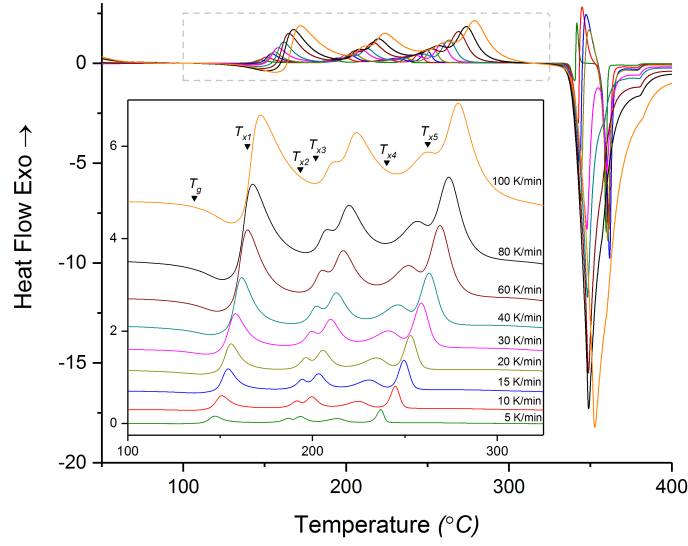


Figure 1: Bulk  $\text{Mg}_{65}\text{Zn}_{30}\text{Ca}_5$  relaxed at  $120^{\circ}\text{C}$  for 10 minutes and heated at various heating rates. The insert stacks the differential scanning calorimetry (DSC) curves and labels the  $T_g$  and  $T_x$ es of the  $100\text{K}/\text{min}$  sample.

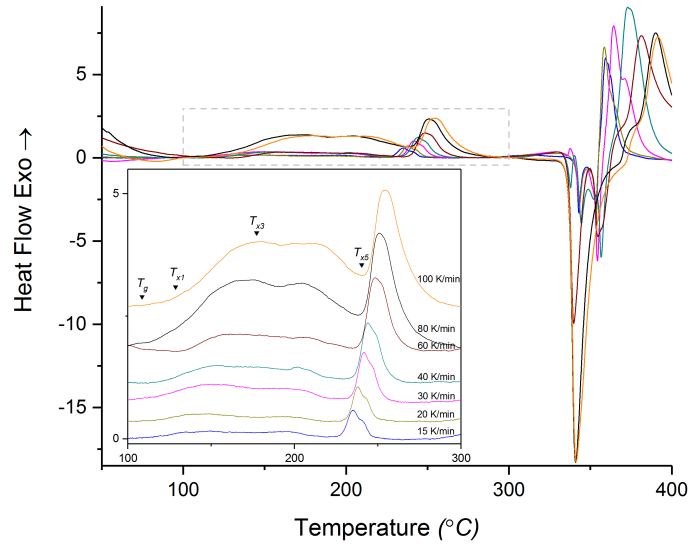


Figure 2: Unrelaxed film  $\text{Mg}_{65}\text{Zn}_{30}\text{Ca}_5$  heated at various heating rates. The insert stacks the DSC curves and labels the  $T_g$  and  $T_x$ es of the  $100\text{K}/\text{min}$  sample.

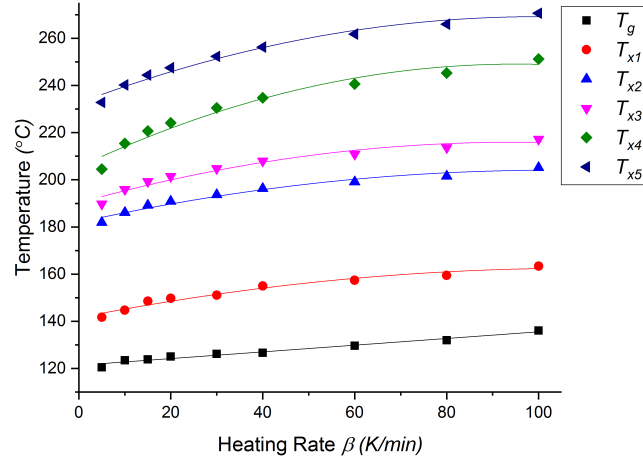


Figure 3: The  $T_g$ s and  $T_x$ es of the bulk  $\text{Mg}_{65}\text{Zn}_{30}\text{Ca}_5$  at all heating rates.

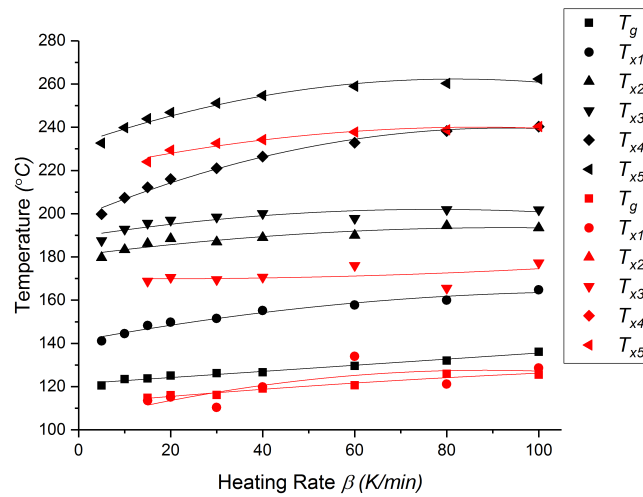


Figure 4: The  $T_g$ s and  $T_x$ es of the bulk and film  $\text{Mg}_{65}\text{Zn}_{30}\text{Ca}_5$  at all heating rates.

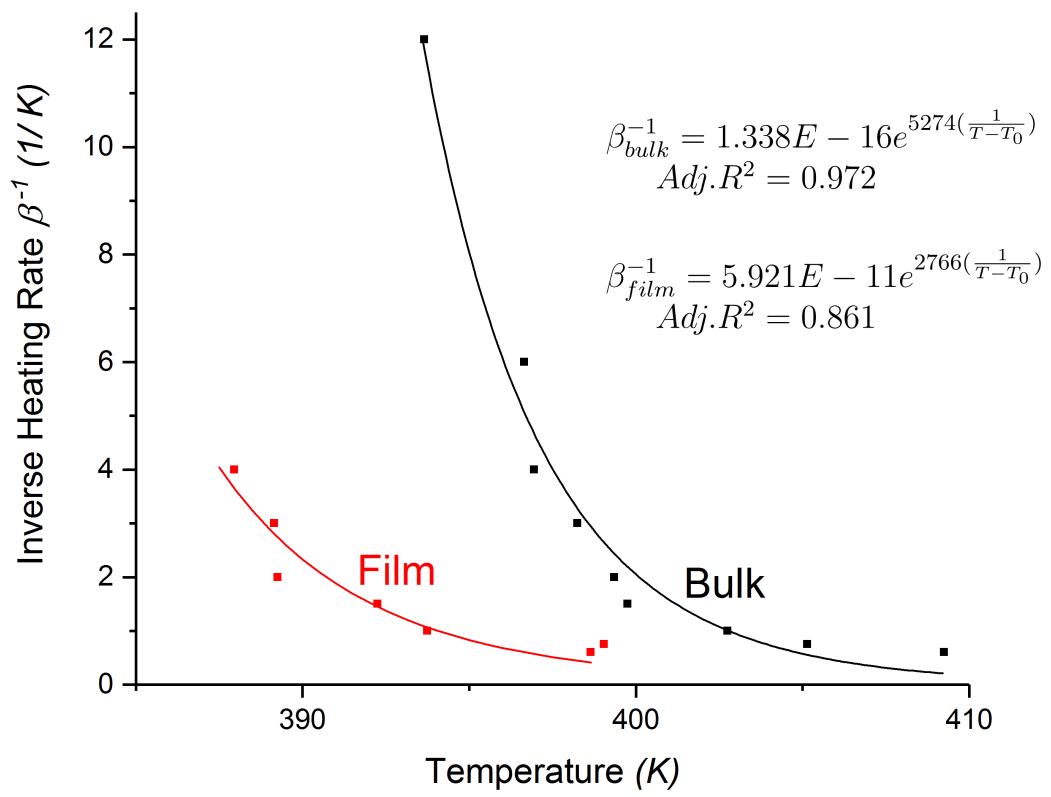


Figure 5: Fitted fragility for the  $Mg_{65}Zn_{30}Ca_5$  system obtained by DSC at various heating rates

m\_mValue

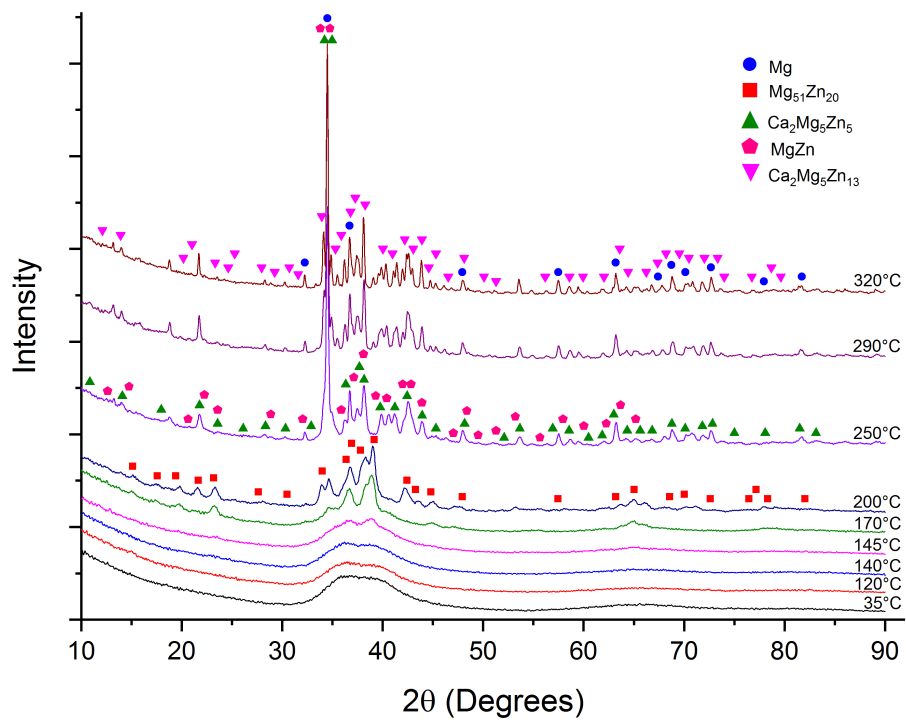


Figure 6: XRD pattern for Bulk  $\text{Mg}_{65}\text{Zn}_{30}\text{Ca}_5$  heated through several crystallization peaks identified from DSC

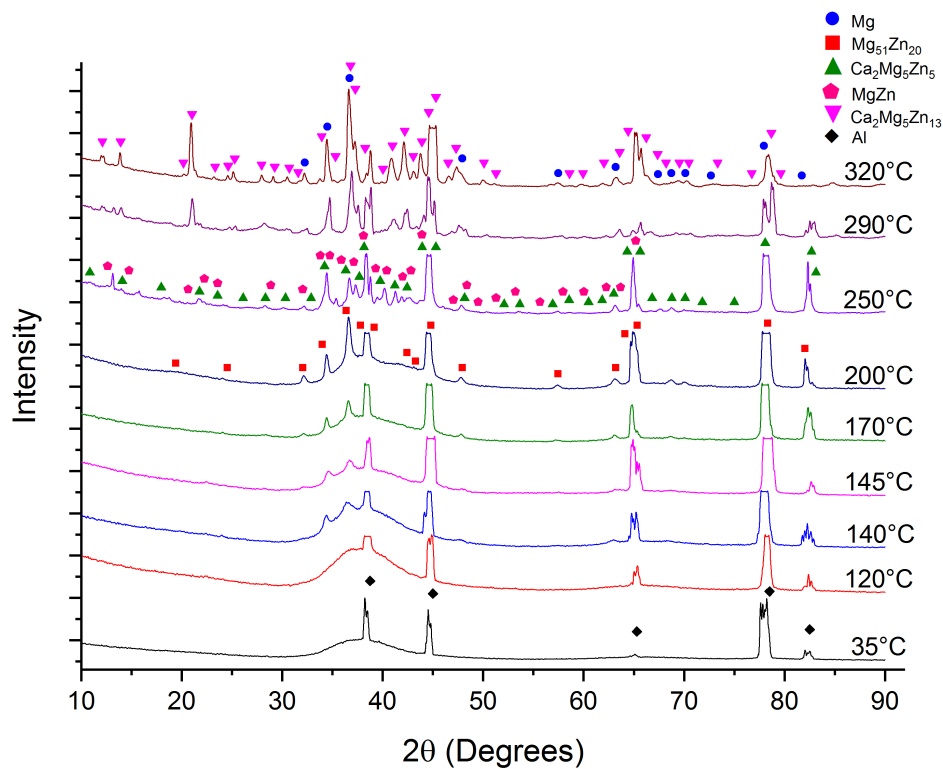
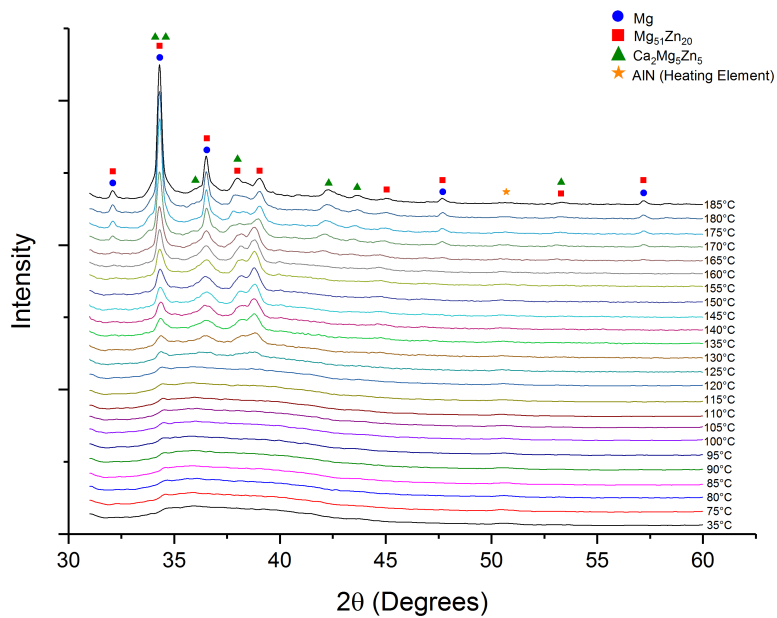
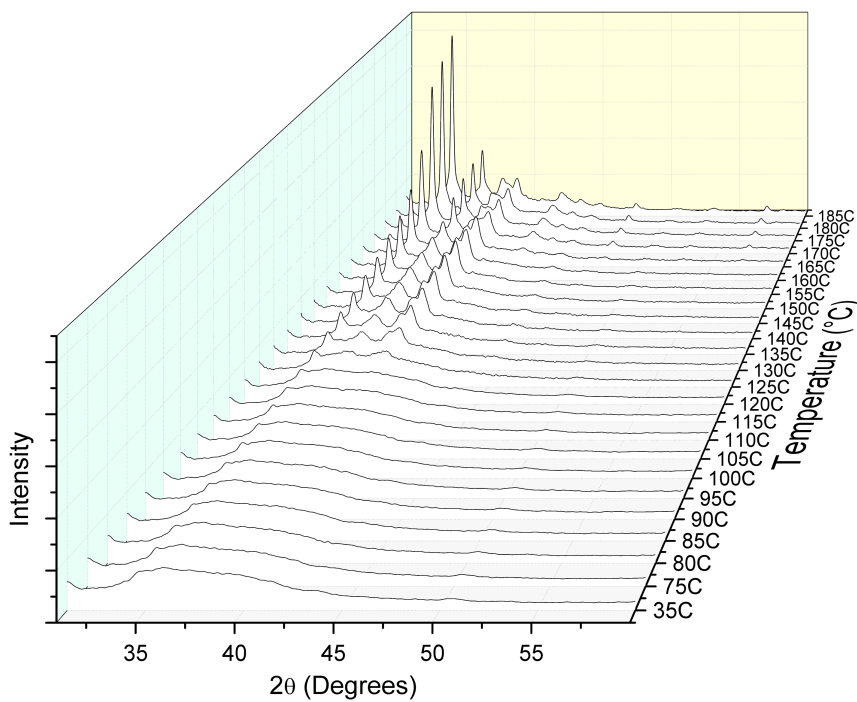


Figure 7: XRD pattern for Film  $\text{Mg}_{65}\text{Zn}_{30}\text{Ca}_5$  heated through several crystallization peaks identified from DSC

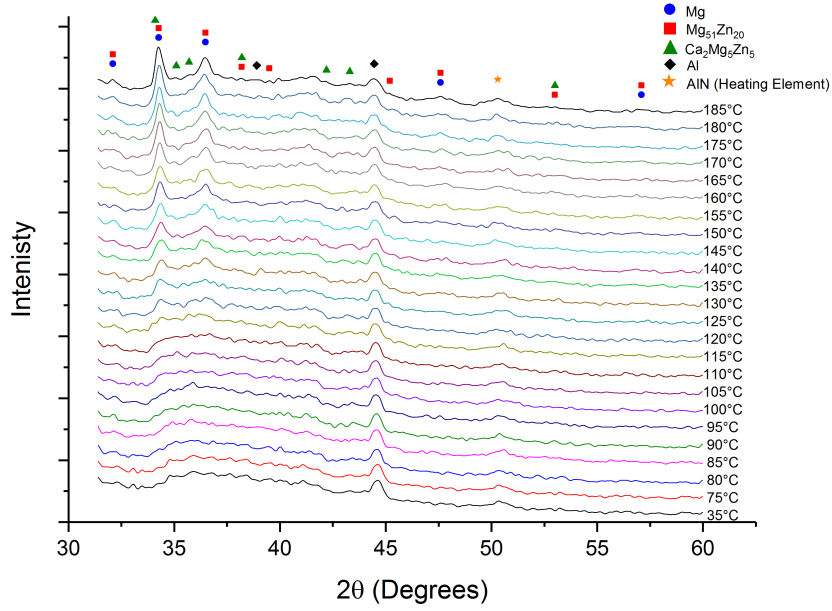


(a)

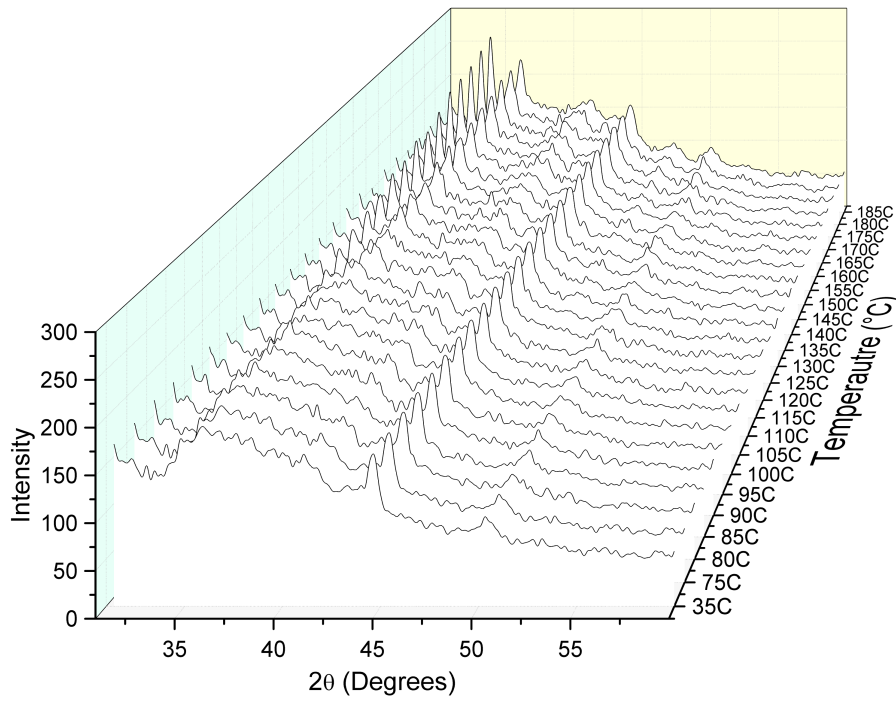


(b)

Figure 8: (a) Stacked X-ray diffraction (XRD) patterns from the incremental heating of bulk  $\text{Mg}_{65}\text{Zn}_{30}\text{Ca}_5$ . (b) Cascading XRD patterns from the incremental heating of bulk  $\text{Mg}_{65}\text{Zn}_{30}\text{Ca}_5$ .



(a)



(b)

Figure 9: (a) Stacked XRD patterns from the incremental heating of film  $\text{Mg}_{65}\text{Zn}_{30}\text{Ca}_5$ . (b) Cascading XRD patterns from the incremental heating of film  $\text{Mg}_{65}\text{Zn}_{30}\text{Ca}_5$ .